Journal of Materials Science: Materials in Medicine (2019) 30:106
https://doi.org/10.1007/s10856-019-6306-y

DELIVERY SYSTEMS

Original Research

An injectable thermosensitive hydrogel for sustained release of apelin-13 to enhance flap survival in rat random skin flap

Wenhao Zheng[1] · Jinwu Wang[1] · Linzhen Xie[1] · Huanguang Xie[1] · Chunhui Chen[1] · Chuanxu Zhang[1] · Dingsheng Lin[1] · Leyi Cai[1]

Received: 5 April 2019 / Accepted: 29 August 2019 / Published online: 9 September 2019

Abstract

With the advantage of handy process, random pattern skin flaps are generally applied in limb reconstruction and wound repair. Apelin-13 is a discovered endogenous peptide, that has been shown to have potent multiple biological functions. Recently, thermosensitive gel-forming systems have gained increasing attention as wound dressings due to their advantages. In the present study, an apelin-13-loaded chitosan (CH)/β-sodium glycerophosphate (β-GP) hydrogel was developed for promoting random skin flap survival. Random skin flaps were created in 60 rats after which the animals were categorized to a control hydrogel group and an apelin-13 hydrogel group. The water content of the flap as well as the survival area were then measured 7 days post-surgery. Hematoxylin and eosin staining was used to evaluate the flap angiogenesis. Cell differentiation 34 (CD34) and vascular endothelial growth factor (VEGF) levels were detected by immunohistochemistry and Western blotting. Tumor necrosis factor-α (TNF-α) and interleukin-6 (IL-6) were assessed by enzyme linked immunosorbent assays (ELISAs). Oxidative stress was estimated via the activity of tissue malondialdehyde (MDA) and superoxide dismutase (SOD). Our results showed that CH/β-GP/apelin-13 hydrogel could not only reduce the tissue edema, but also improve the survival area of flap. CH/β-GP/apelin-13 hydrogel also upregulated levels of VEGF protein and increased mean vessel densities. Furthermore, CH/β-GP/apelin-13 hydrogel was shown to significantly inhibit the expression of TNF-α and IL-6, along with increasing the activity of SOD and suppressing the MDA content. Taken together, these results indicate that this CH/β-GP/apelin-13 hydrogel may be a potential therapeutic way for random pattern skin flap.

These authors contributed equally: Wenhao Zheng, Jinwu Wang, Linzhen Xie

These authors contributed equally: Dingsheng Lin, Leyi Cai

✉ Leyi Cai
caileyi@wmu.edu.cn

[1] Department of Orthopaedic Surgery, The Second Affiliated Hospital and Yuying Children's Hospital of Wenzhou Medical University, 325000 Wenzhou, China

Graphical Abstract

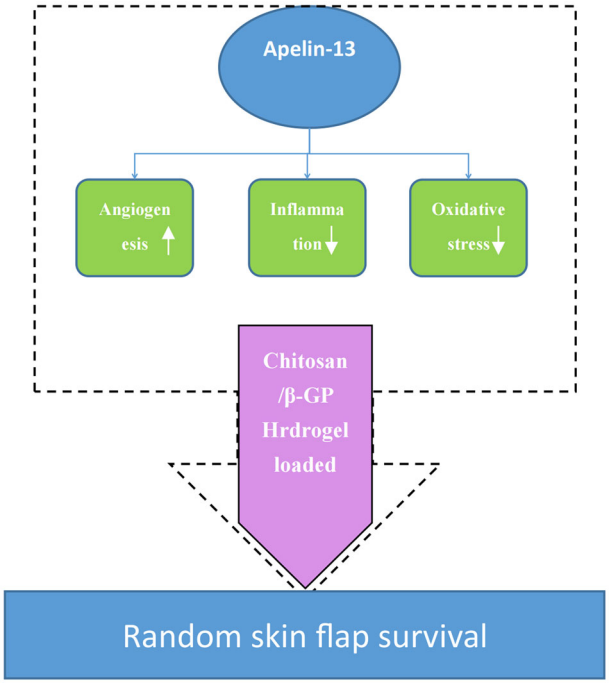

1 Introduction

Soft tissue defect is a common and difficult problem in plastic and reconstructive surgery, which is caused by traumatic or cancer-associated deformities. Due to its simple procedure, skin random flap is widely used for transplantation to functional and aesthetic reconstruction by plastic surgeons, especially for tissue repair [1, 2]. Though, the length-to-width ratio of such flaps cannot be increased beyond 1.5:1 to 2:1 [3]. Thence, necrosis of the flap distal end (partial or complete) is a common phenomenon after surgery. A growing body of studies have suggested that insufficient blood flow, ischemia-reperfusion injury, vascular congestion, inflammatory response and oxidative stress contribute to flap necrosis [4–6]. Therefore, acceleration of angiogenesis and inhibition of oxidative stress as well as the inflammatory mediators are the main effective strategies to enhance the survival of random pattern skin flap.

Apelin was primordially separated from the tissue samples collected from bovine's stomach. There are many kinds of bioactive forms of apelin derived from a 77-amino acid prepropeptide precursor [7–9]. Among these, apelin-13 possesses the strongest biological activities [10, 11]. It has been reported that intranasal administration of apelin-13 following an ischemic stroke ameliorated such ischemic injury by restoring local cerebral blood flow, promoting angiogenesis and reducing inflammatory activities in mice [11]. In addition to that, apelin-13 was found to protect the brain from ischemia/reperfusion injury via a mechanism involving activation of ERK1/2 and PI3K/Akt signaling pathways [12]. Through the RISK-GSK-3β-mPTP pathway, apelin-13 similarly protected the heart against ischemia/reperfusion injury [13]. Therefore, we hypothesized that apelin-13 might to some extent improve the random skin flaps survival. However, due to the short half-live of apelin-13, prolonged treatment is recommended so as to maintain long-term efficacy. Hence, to resolve this challenge, attempts towards developing control-release drug platforms that ensure prolonged release of apelin-13 are encouraged.

In virtue of easy preparation, easy application, low toxicity, low cost and controlled release, hydrogel exhibits special advantages, is widely believed to be an employed carrier in drug-controlled release [14, 15]. Because of distinct antioxidation and excellent biocompatibility, chitosan (CH) is in widespread use among the field of tissue engineering. As a prospective biomolecule, chitosan has aroused wide attention from researchers engaged in tissue regeneration and repair field [16]. Chitosan and β-sodium glycerophosphate (β-GP) are the main ingredients of hydrogel that is frequently used in biomedical field [17]. When combined with β-GP, chitosan is able to form a thermosensitive

hydrogel, capable of staying as a liquid at low temperatures and as a semisolid at higher temperatures. β-GP shields chitosan chains from water when in acidic conditions. This is based on its ability to form hydrogen bonds which increases the solubilization of chitosan when exposed to high pH and low temperatures conditions [18]. At high temperatures, the hydrogen bonds formed among chitosan chains and water molecules are dissociated, and this enhances the chitosan-chitosan hydrophobic bonding, leading to phase transition from liquid to gel [19]. The resultant semisolid hydrogel supports the transferred cells by simulating the extracellular matrix thereby providing suitable cell survival environment [20, 21].

In this study, apelin-13 was loaded into a CH/β-GP system to form a novel thermosensitive hydrogel (CH/β-GP/apelin-13) for the treatment of a rat random pattern skin flap model. CH/β-GP/apelin-13 was first prepared and its drug release rate, degradation rate and rheology were investigated. Following this, CH/β-GP/apelin-13 was assayed for its potential anti-inflammatory, antioxidant and promoting angiogenesis effects as well as the underlying mechanism on a rat random pattern skin flap model.

2 Experimental procedures

2.1 Materials

Chitosan (degree of deacetylation ≥95%; average molecular weight, 650 kDa), β-glycerophosphate (β-GP) and apelin-13 (Sigma Chemical Co. (USA), anti-VEGF and Anti-CD34 (Bioss Biotechnology (Beijing, China), β-actin and HRP-conjugated IgG second antibodies (Santa Cruz Biotechnology, California, USA). SOD and MDA test kits, IL-6, and TNF-α ELISA kits (Nanjing Jiancheng Biology Institution, China).

2.2 β-glycerophosphate solution (GP) and dialyzed chitosan solution (CH) preparations

200 mg chitosan was dissolved in 9 ml of aqueous acetic acid (0.1 M), and the insoluble residues were removed by filtration. A dialysis method based on that reported by Kim et al. [19] was then used to reduce the acetic acid content. Briefly, the chitosan solution was placed into a 27-mm dialysis bag (MW: 8000; Biosharp, Hefei, China) in distilled water, and the distilled water was changed daily for a week. The solution was then autoclaved, cooled, and stored at 4 °C for further use. Preparation of GP solutions was done by adding 300 mg of GP to 1 ml water, followed by filtration through 0.22-μm PES syringe filters (Millex™, EMD Millipore, Billerica, MA, USA).

2.3 Preparation of apelin-13 and determination of apelin-13 content

Apelin-13 (400 mg) was dissolved in 100 ml deionized water in a 200 ml glass vial with a magnetic bar for 10 min, then centrifuged at $1000 \times g$ for 5 min. Subsequently, the supernatants were harvested and freeze-dried in a Labconco Freeze Dry System (USA) to recover the water soluble apelin-13.

Apelin-13 concentration was measured using a UV-Vis spectrophotometer method (Orion™ AquaMate 8000; Thermo Fisher Scientific, Inc., USA) at 425 nm. First, a standard curve of apelin-13 in dimethyl sulfoxide (DMSO; 0–10 μg/ml) was prepared under identical conditions. Subsequently, 1 mg of water soluble apelin-13 was dissolved in 5 ml DMSO by gently shaking for 24 h at 37 °C away from light. The solution was then subjected to centrifugation at $14{,}000 \times g$ for 3 min, and the obtained apelin-13-containing DMSO supernatant was collected to determine the apelin-13 content in the water soluble apelin-13.

2.4 Preparation of CH/β-GP hydrogel and apelin-13-loaded CH/β-GP hydrogel (CH/β-GP/apelin-13 hydrogel)

CH/β-GP hydrogel was prepared by adding β-GP drops (1 ml) to 9 ml dialyzed chitosan under gentle stirring in ice bath [22, 23]. The chitosan and β-GP concentrations of the CH/β-GP hydrogel were 2% (w/v) and 3% (w/v), respectively. CH/β-GP/apelin-13 hydrogel was prepared via simple mixing method. First, 200 mg of water soluble apelin-13 was dissolved into 1 ml deionized water and then added to 9 ml of dialyzed chitosan solution under mechanical stirring. At last, CH/β-GP/apelin-13 hydrogel was prepared by adding 1 ml β-GP solution dropwise to CH/apelin-13 solution (10 ml) in an ice bath as above. Control hydrogel was made analogously avoiding adding apelin-13 solution. The obtained hydrogels were frozen at −20 °C followed by lyophilization for 24 h, and then preserved in an airtight containers or use.

2.5 Examination of hydrogels by electron microscopy

The CH/β-GP/apelin-13 hydrogel morphology was assessed using a scanning electron microscope (SEM; FEI Quanta 200; Thermo Fisher Scientifc, Eindhoven, Netherlands) at an accelerating voltage of 30 kV. The CH/β-GP/apelin-13 hydrogel was prepared at 37 °C for 4 h, placed into distilled water at 37 °C for 24 h, and then lyophilized in the Labconco Freeze Dry System (Labconco) [19]. Dry samples were placed on double-sided carbon tape, gold-sputtered and mounted on the SEM stage before scanning.

2.6 The release profile of apelin-13 from the hydrogel in vitro

The drug release profile of CH/β-GP/apelin-13 hydrogel was assessed by HPLC. In brief, 4 ml of dialyzed chitosan, 0.5 ml of 30% β-GP and 100 mg of water soluble apelin-13 were mixed as above and placed into 6-well plates. The plate was cultures for 10 min at 37 °C to induce sol-gel transition of the CH/β-GP/apelin-13 hydrogel. Subsequently, 3 ml PBS (0.01 M, pH 7.35) were pipetted to each well and the plates were gently shaken at 37 °C. The supernatants were pipetted out at predetermined time points and replaced with the same volume of pre-warmed PBS. After spinning at 13,000 × *g* for 10 min, the supernatants were collected and kept at −20 °C for further tests. Released apelin-13 was quantified at 425 nm using HPLC (Waters Co., Milford, MA, USA).

2.7 Degradation behavior of CH/β-GP/apelin-13 hydrogel in vitro

The degradation rate of CH/β-GP/apelin-13 was determined using an enzymatic degradation method. In brief, CH/β-GP/apelin-13 was prepared in a 6-well plate, frozen overnight (−80 °C) and then lyophilized at −35 °C (VirTis AdVantage Wizard 2.0; SP Scientific, Stone Ridge, NY, USA) for 3 days. The freeze-dried hydrogel was weighed (W0) and then placed in PBS containing 500–1000 U/ml of lysozyme (kept in a 37 °C water bath). At specific time intervals, the hydrogels were carefully retrieved, washed, frozen, lyophilized and weighed (Wt). The degradation rate of CH/β-GP/apelin-13 was determined based on its reduction in weight, according to the following formula: Weight loss (%) = [(W0 – Wt)/W0] × 100%. The procedure was conducted in triplicatel.

2.8 Rheological behavior of CH/β-GP/apelin-13 hydrogel

Sol-gel transition characteristics of the CH/β-GP/apelin-13 were studied by rheometry. In brief, 1 ml of the CH/β-GP/apelin-13 was individually placed into the rheometer, and the rheological properties of the sample were evaluated between 10 °C and 40 °C at constant heating rate of 1 °C/min. The viscous modulus G″ (Pa) as well as elastic modulus G′ (Pa) dynamics were observed for each temperature at a fixed frequency of 1 Hz.

2.9 Animals

In total, 60 healthy Sprague-Dawley rats (male, body weight 220~250 g) were acquired from the Animal center of Wenzhou Medical University (WMU, China) (license no.SCXK [Zhe] 2005–0061). The animal operation and treatment conformed to the Guide for the Care and Use of Laboratory Animals of China National Institutes of Health. All procedures were approved by the Animal Care and Use Committee of WMU (wydw 2012–0079). Upon arrival, animals were individually caged and kept in rooms where light (12-h/12-h light/dark), humidity, and temperature (22 ± 2 °C) were controlled. All experimental animals were freely given tap water and standard chow.

2.10 Animal model of random skin flap

Adapted to one overnight, all experimental animals were shaved and sterilized before surgery. The surgical operation was completed under general anesthesia. The anesthesia of all rats was achieved via an intraperitoneal injection with 40 $mg \cdot kg^{-1}$ sodium pentobarbital. The pinch flexion/withdrawal experiment was used to determine the adequate anaesthesia. A modified McFarlane flap (3 × 9 cm; Fig. 1a) was created on every experimental animal. To ensure accurate positioning, the proximal end of the flap was on the margin of the iliac crest as a maker. To reduce bacterial infections, all instruments and surgical procedures are sterile. Sacral arteries in both sides were sectioned completely to ensure no axial vessel was incorporated into the flap (Fig. 1c). Following each model was dissociated from the deep fascia completely, all flaps were repositioned into initially position with 4–0 silk (Fig. 1d).

2.11 Experimental animal design

60 rats were randomly split up into two groups ($n = 30$ in each group): control hydrogel group and apelin-13 hydrogel group. The control hydrogel group ($n = 30$) received intradermal injection of CH/β-GP hydrogel solution (0.1 ml/kg each point) while the apelin-13 hydrogel group ($n = 30$) received intradermal injection of CH/β-GP/apelin-13 hydrogel solution (0.1 ml/kg each point) in the proximal, middle and distal areas of the flap after the surgical procedure. The hydrogel was injected in the center of a 1 × 1 cm area using a latticed silicone sheet that contained 27 points of injection. All rats were sacrificed by cervical dislocation at day 7.

2.12 Flap survival assessment

The random skin flap was classified to three identical areas: the proximal of flap as Area I, intermediate of flap as Area II, and distal of the flap as Area III. The macroscopic changes (flap appearance, color, texture, and hair status) of

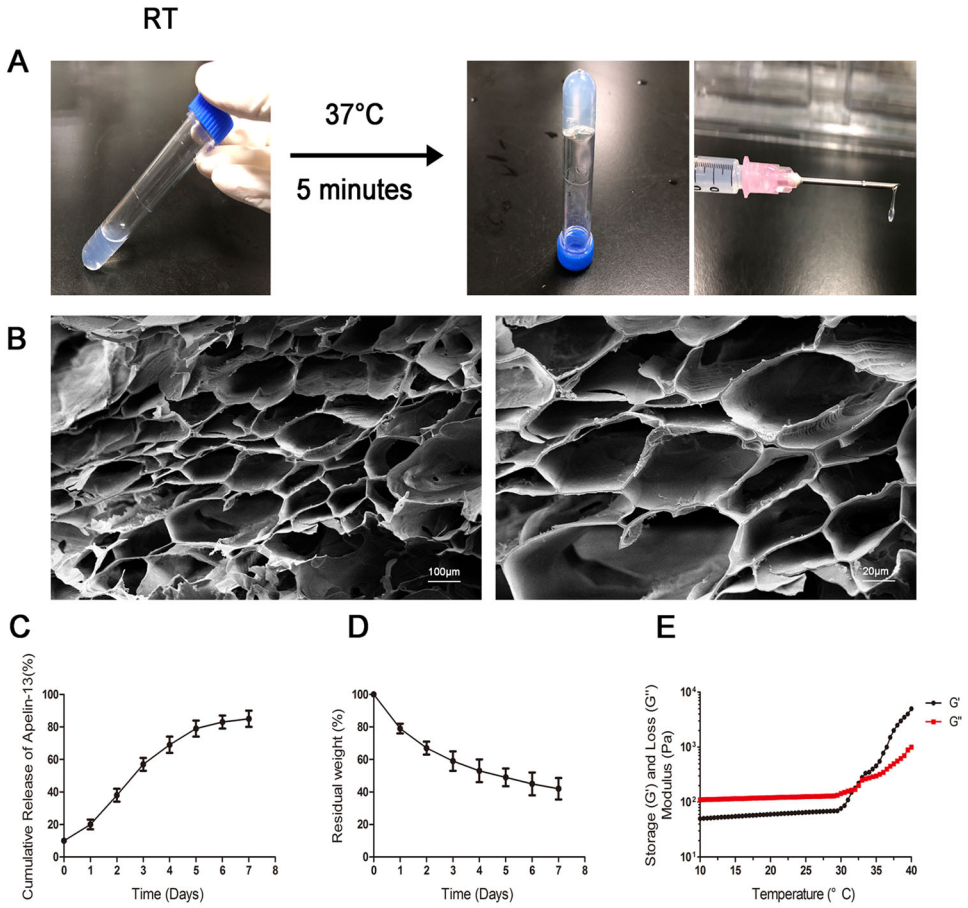

Fig. 1 Characterization of CH/β-GP/apelin-13 hydrogel. **a** A photo showing the temperature-triggered sol (left, room temperature) to gel (right, 37 °C for 5 min) transition; **b** scanning electron micrographs of the pore architecture of CH/β-GP/apelin-13 hydrogel; **c** in vitro apelin-13 release behavior of CH/β-GP/apelin-13 hydrogel; **d** in vitro degradation profile of CH/β-GP/apelin-13 hydrogel; **e** rheological analysis of the CH/β-GP/apelin-13 solution. The arrow head indicates the transition point where G′ (elastic modulus) outweighs G″ (viscous modulus)

the random skin flap were evaluated. We measured surviving and total flap areas on transparent cellophane sheets and calculated flap survival percentages as survival area × 100/total area (survival and ischaemic).

2.13 Determination of tissue edema

Flap tissue edema represented through its water content. On the 7th day, we harvested and weighed flap tissues and then autoclaved at 50 °C to dry them. The specimens were weighed daily for 2 days consecutively to achieve a stable weight. The following formula was applied to calculate the % of water content: Tissue % water content = ([wet weight − dry weight]/wet weight) × 100%.

2.14 Laser Doppler imaging

All animals underwent laser Doppler perfusion imaging at room temperature on the last day. The parameters of the instrument were as follows: 633 nm laser wavelength, 55 cm scan and 5 min duration. The results were quantified by the MoorLDI Review V6.1 software. The measurement would repeat three times for every rat and the mean value was calculated after three times repeat [24].

2.15 Immunohistochemical staining

All flap zones were subjected to immunohistochemical VEGF and CD34 staining with the streptavidin-peroxidase way; we blocked all slices with routine goat serum at 25 °C for 20 min; followed by addition of 50 μL amounts of primary VEGF antibodies (1:100) and CD34 antibodies (1:100) followed by hatched at 4 °C for 24 h; rewarmed the slides to 37 °C for 50 min; washed them with PBS; added 50 μL amounts of goat anti-rat antibodies (1:50) after which they were incubated for 1 h at 37 °C; washed the slices with distilled water; added 3,3′ N-diaminobenzidine tetrahydrochloride (for colour development) followed by counterstain for 5 min. VEGF expression was identified using the inverted BH51 microscope at ×400 magnification in five fields/slice for each group. All images were carefully analyzed through the software Image-Pro Plus ver. 6.0. Afterwards, integral absorbance (IA) values were used as a measure of VEGF and CD 34 level.

2.16 H&E staining

After sacrifice, three 1 × 1-cm central samples were collected from every area, which were the fixed in 4% (v/v) paraformaldehyde, followed by embeddedment in paraffin. Then, samples were made into slices of 4-μm thickness. Slides were observed under a light microscope with 200 magnification (Olympus Corporation, Japan) by two separate physicians. Edema, granulation thickness, neutrophil numbers and microvessel numbers/mm^2 (an indicator of microvascular density [MVD]) were evaluated.

2.17 Protein quantification by Western blotting

At 7 days post-operation, we obtained specimens (1 × 1-cm) from area II and preserved them at −80 °C. These specimen was lysed to extract proteins, followed by determining the protein concentration using BCA assay kits. 70 μg amounts of protein was separated on a 12% SDS-PAGE after which they were electrotransferred to PVDF membrane. 5% non-fat milk was used to block non-specific binding on the membrane by incubating the membrane for 2 h at room temperature. This was followed by incubation of the membrane with anti-VEGF (1:1000), CD 34 (1:1000) and β-actin (1:1000) antibodies. After that, the membrane was incubated with a HRP-conjugated secondary antibody (1:3000) for 2 h at room temperature. In the final step, the membrane was developed with enhanced chemiluminescence (ECL) kit and analysed using Quantity One software.

2.18 Quantification of malondialdehyde (MDA level and Superoxide dismutase (SOD) activity

At 7 days postoperatively, flap specimen (0.5 × 0.5 cm) of each group was acquired from districts between Area II and the other areas, weighed, and muscle tissues prepared as 10% volume fractions after homogenisation on ice bath. The enzymatic xanthine oxidase test was utilized to estimate SOD activity whereas thiobarbituric acid test was used to determine the malondialdehyde (MDA) content at 95 °C [25, 26].

2.19 Estimation of IL-6 and TNF-α levels

Commercial ELISA kits were utilized to estimate IL-6 and TNF-α levels in serum following the manufacturer's protocols.

2.20 Statistical analysis

Data are presented as mean ± SD. Comparisons between groups were analyzed by SPSS version 18.0 software and statistical significance was analyzed using one-way analysis of variance (ANOVA). Values with $P < 0.05$ were considered statistically significant.

3 Results

3.1 Physicochemical characterization of CH/β-GP/apelin-13 hydrogel

3.1.1 Micro and macro appearance of CH/β-GP/apelin-13 hydrogel

SEM analyses was employed to estimate the pore architecture in the CH/β-GP/apelin-13 hydrogel, which revealed that most of CH/β-GP/apelin-13 hydrogel possessed pores >100 μm (Fig. 2b). The macro appearance and the sol-gel transition process are depicted in Fig. 2a; the test tube on the left shows CH/β-GP/apelin-13 hydrogel under room temperature while the test tube on the right shows the gel phase of CH/β-GP/apelin-13 hydrogel when placed at 37 °C for 5 min.

3.1.2 In vitro apelin-13 release behavior of CH/β-GP/apelin-13 hydrogel

An apelin-13 release profile of the CH/β-GP/apelin-13 hydrogel was generated using a HPLC method, as shown in Fig. 2c. It was observed that apelin-13 was released slowly in a sustained manner rather than in a rapid-burst release; 85.7 ± 5.6% of the apelin-13 was released within 1 week. This apelin-13 release profile indicated the potential of the CH/β-GP/apelin-13 hydrogel composite as an in situ gel system with sustained drug release capacity.

3.1.3 Degradation behavior of CH/β-GP/apelin-13 hydrogel in vitro

To evaluate the stability of CH/β-GP/apelin-13 hydrogel when applied on random flaps, the degradation profile of CH/β-GP/apelin-13 hydrogel was determined by an enzymatic degradation method. As shown in Fig. 2d. 58.3 ± 6.6% of the CH/β-GP/apelin-13 hydrogel was degraded within 7 days.

3.1.4 Rheological properties of CH/β-GP/apelin-13 hydrogel

Figure 2e shows the alterations in the viscous modulus (G") and elastic modulus (G′) of the CH/β-GP/apelin-13 hydrogel as functions of temperature. The sol-gel transition took place at around 32 °C, which was characterized by a marked increase in G′. Following this, G′ showed a stable increase as a function of temperature while G"showed little increase. The higher G′ value compared with G″ indicated successful sol-gel transition.

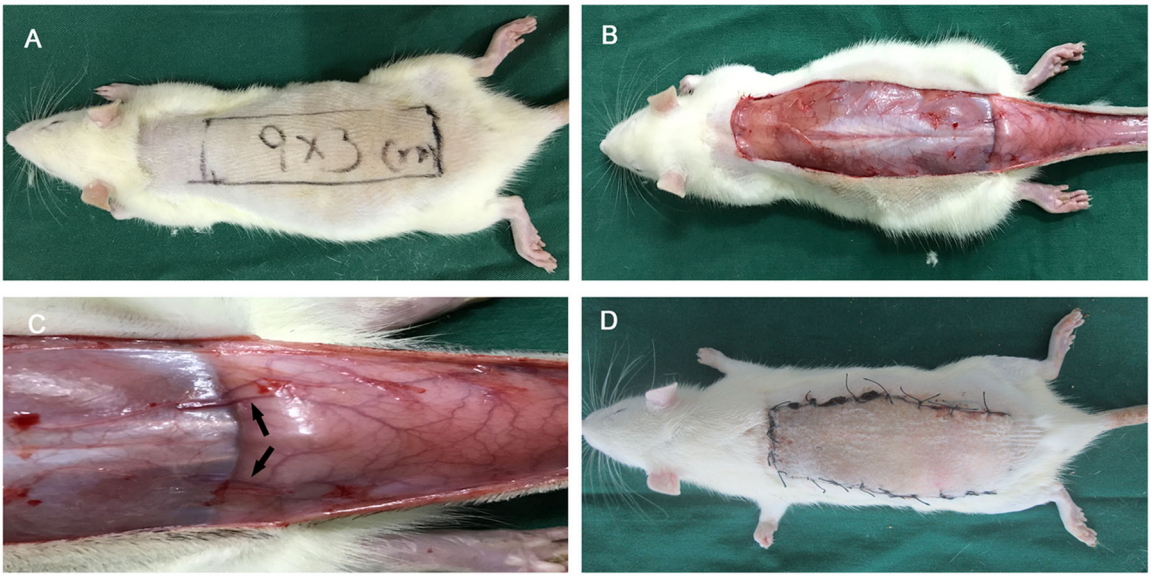

Fig. 2 Random skin flap model. **a**, **b** A modified McFarlane flap model (3 × 9 cm) was created in the dorsum of each rat. **c** Both sacral arteries near the base of the flap were sectioned systematically. **d** Flap was sutured back to its original position with continuous 4–0 silk sutures

3.2 Effect of CH/β-GP/apelin-13 hydrogel on tissue edema and skin flap survival

All flaps were monitored by the same observer from days 1 to 7 postoperatively, and colour, elasticity, and necrosis recorded. One day after surgery, all flaps were pale and swollen. All flaps were purple and oedematous in Area III, indicating distal ischaemia. On day 3, these regions underwent necrosis, evidenced by the appearance of dark brown nidi. On day 7 postoperatively, all flaps exhibited clearly-dividing line between surviving and ischemia regions. The ischemia areas were scab, harden, inanimate; the surviving areas were ruddy, pastel, active (Fig. 3c, d). A significant between-group difference in terms of survival area was evident: 73.7 ± 7.1% (apelin-13 hydrogel group) and 46.3 ± 7.2% (control hydrogel group) with $P < 0.01$ (Fig. 3e). As shown in Fig. 3c, d, f, % of water content of the tissue was markedly lower in apelin-13 hydrogel group (44.0 ± 7.0%) compared to that of the control hydrogel group (63.3 ± 7.6%) ($P < 0.05$), indicating that the tissue inflammatory edema of the rat random skin flap model was strikingly decreased by the CH/β-GP/apelin-13 hydrogel treatment.

3.3 Effect of CH/β-GP/apelin-13 hydrogel on the blood-flow of the flap

On the day 7, we used the Laser Doppler system to estimate the blood-flow situation of all flaps. The flow rates in middle area were 97.0 ± 23.3 (control hydrogel group) and 462.7 ± 53.1 (apelin-13 hydrogel group) perfusion units, respectively, which suggests that the blood flow in the apelin-13 hydrogel group was remarkably greater than that in control (Fig. 4, $P < 0.01$).

3.4 Influence of CH/β-GP/apelin-13 hydrogel on histopathologic examination and vascularization

To evaluate the effects of CH/β-GP/apelin-13 hydrogel on granulation tissue thickness, oedema, and neutrophil infiltration, flap sections were HE-stained. The distal areas of all flaps were morphologically similar. As shown in Fig. 5, on day 7, all flaps revealed analogous changes, including structural damage, edema and seep inflammatory cells. Of all images, 90% exhibited muscle fibre degeneration and necrosis. When analyzed the Area II, compared with the control group, the apelin-13 hydrogel group displayed larger fibroblast multiplication, covered with fresh granulation soft tissue, less oedema, bushier fascia haemorrhage, more extensive inflammatory cells infiltration and more neovascularization (Fig. 5b, d). Besides, the mean vessel densities (MVDs) for area I in apelin-13 hydrogel and control hydrogel group were 47.3 ± 6.4 and 44.3 ± 4.0/mm^2, respectively ($P > 0.05$). The MVDs of area II were 39.0 ± 5.6 and 21.3 ± 4.7/mm^2 in apelin-13 hydrogel group and control hydrogel group respectively (Fig. 5e). This statistically significant difference was ($P < 0.01$).

3.5 Effect of CH/β-GP/apelin-13 hydrogel on CD34 and VEGF expression

Through immunohistochemistry, the expression of VEGF and CD 34 was evaluated. According to IA value of CD 34,

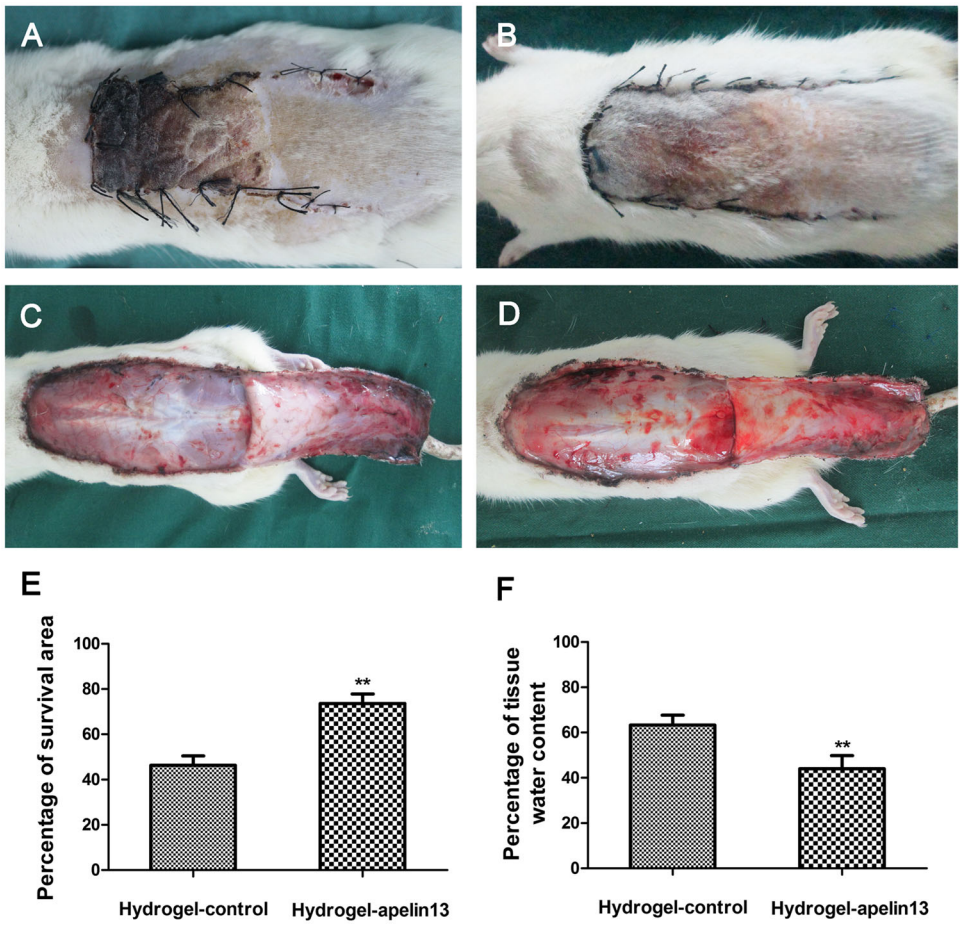

Fig. 3 Effect of CH/β-GP/apelin-13 hydrogel on skin flap survival and tissue edema. **a**, **b** Digital photographs of flap survival in the control hydrogel group and apelin-13 hydrogel group were taken on day 7. **c**, **d** Digital photographs of the inner side of the skin flap were taken from each group to show the degree of tissue edema. **e** Flap survival percentages for each group were then quantified and analyzed. **f** Quantification and analysis of the tissue water content percentages in each group are shown. $*p < 0.05$ and $**p < 0.01$ in comparison with the control group. Data represent mean values ± SD, $n = 6$ per group

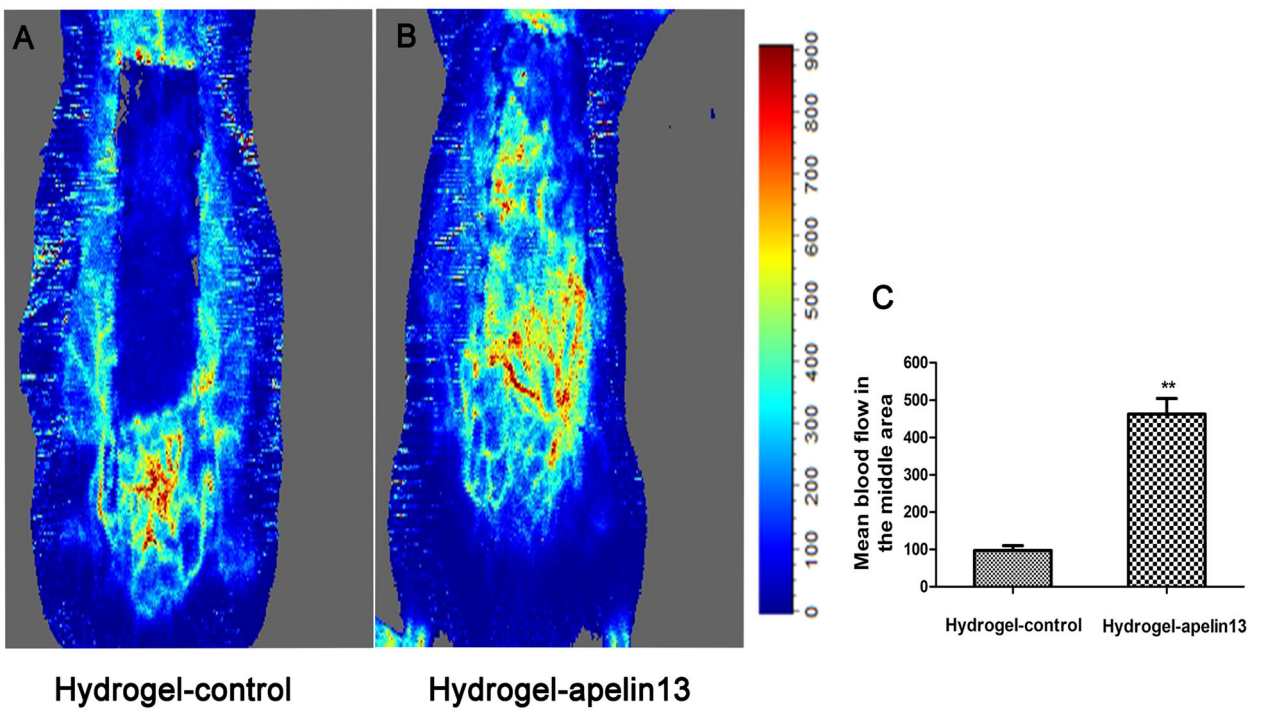

Fig. 4 Effect of CH/β-GP/apelin-13 hydrogel on the blood flow of the flap. **a**, **b** The blood perfusion on day 7 in the two groups. **c** Mean blood flow of area II in the gap in the two groups measured by laser Doppler imaging at day 7 after surgery. $*p < 0.05$ and $**p < 0.01$ in comparison with the control group. Data represent mean values ± SD, $n = 6$ per group

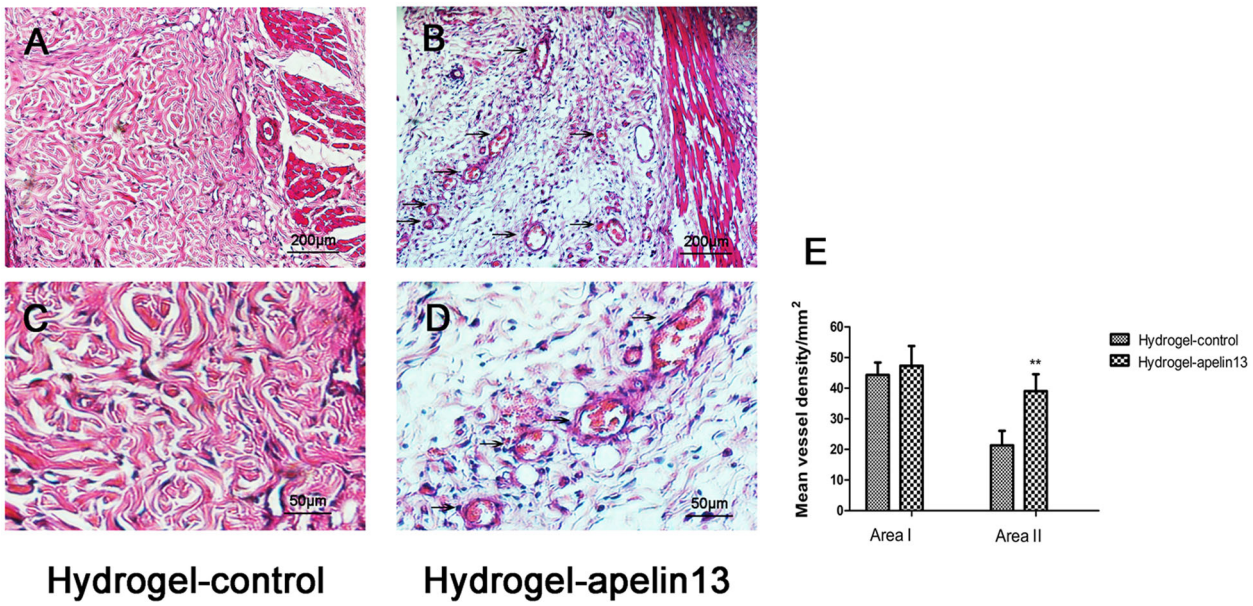

Fig. 5 Effect of CH/β-GP/apelin-13 hydrogel on histopathologic examination and vascularization. **a**–**d** Neovascularization in the control hydrogel group and apelin-13 hydrogel group by hematoxylin and eosin staining. **e** Microvascular density (MVD) reflects the number of microvessels per unit area (mm^2). $*p < 0.05$ and $**p < 0.01$ in comparison with the control group. Data represent mean values ± SD, $n = 6$ per group

we observed that CD 34 levels were much higher in apelin-13 hydrogel group (3740.0 ± 535.1) as compared to the control hydrogel group (1326.3 ± 339.2) ($P < 0.01$, Fig. 6a, c). Along with this, the VEGF expression was also higher in the apelin-13 hydrogel group (1455.0 ± 236.2) than in the control hydrogel group (566.3 ± 178.6) ($P < 0.01$, Fig. 6b, d). Western blot results also demonstrated higher expression of VEGF and CD34 in the apelin-13 hydrogel group relative to control group ($P < 0.01$, Fig. 6e–g).

3.6 Effects of CH/β-GP/apelin-13 hydrogel on proinflammatory cytokines

Measurement of proinflammatory cytokines, including TNF-α and IL-6, was performed to assess the response of inflammation. CH/β-GP/apelin-13 hydrogel was noticed to significantly decrease the levels of TNF-α (76.7 ± 20.8 pg/mL) relative the control group (142.40 ± 24.9 pg/mL) (Fig. 7a). The levels of IL-6 following CH/β-GP/apelin-13 hydrogel administration (48.3 ± 16.1 pg/mL) were also reduced in comparison with the controlled (99.0 ± 18.2 pg/mL) (Fig. 7b). To this end, these data indicate that CH/β-GP/apelin-13 hydrogel reduces the release of proinflammatory cytokines in the flap.

3.7 Influence of CH/β-GP/apelin-13 hydrogel on oxidative stress

Measurement of the antioxidant SOD and the lipid peroxidation product MDA are shown in Fig. 7c, d. In term of mean SOD activity, apelin-13 hydrogel group showed higher grades relative to control group (66.7 ± 6.7 $u \cdot mg^{-1}$ $protein^{-1}$ and 27.7 ± 6.8 $u \cdot mg^{-1}$ $protein^{-1}$, $P < 0.01$; Fig. 7c). Also, the apelin-13 hydrogel group (44.3 ± 10.0 $nmol \cdot mg^{-1}$ $protein^{-1}$) exhibited significantly lower mean MDA content compared to the control group (66.0 ± 9.5 $nmol \cdot mg^{-1}$ $protein^{-1}$, $P < 0.01$, Fig. 7d).

4 Discussion

Random skin flap necrosis extends the hospital stay, increases treatment costs, and triggers more surgical interventions. However, necrosis, especially in the distal regions of random flaps, compromises flap utility [27, 28]. Apelin-13 is a discovered endogenous peptide, that has been shown to have potent multiple biological functions [29]. It has been reported that apelin-13 exerts pivotal role in angiogenesis. For instance, apelin-13 could promote angiogenesis, maintain local cerebral blood flow and inhibit inflammatory activities in ischemic stroke mice [11]. Besides, apelin-13 could reverse the ischemia/reperfusion injury of heart and brain via the ERK1/2, PI3K/Akt and RISK-GSK-3β-mPTP pathway [12, 13]. The present study is aimed to develop a novel apelin-13-loaded CH/β-GP hydrogel with the capacity to facilitate the survival of rats with random pattern skin flap. As displayed by the results, the thermo-sensitive hydrogel was successfully prepared and its drug release rate, degradation rate and rheological properties were determined. Besides, our results showed that apelin-13

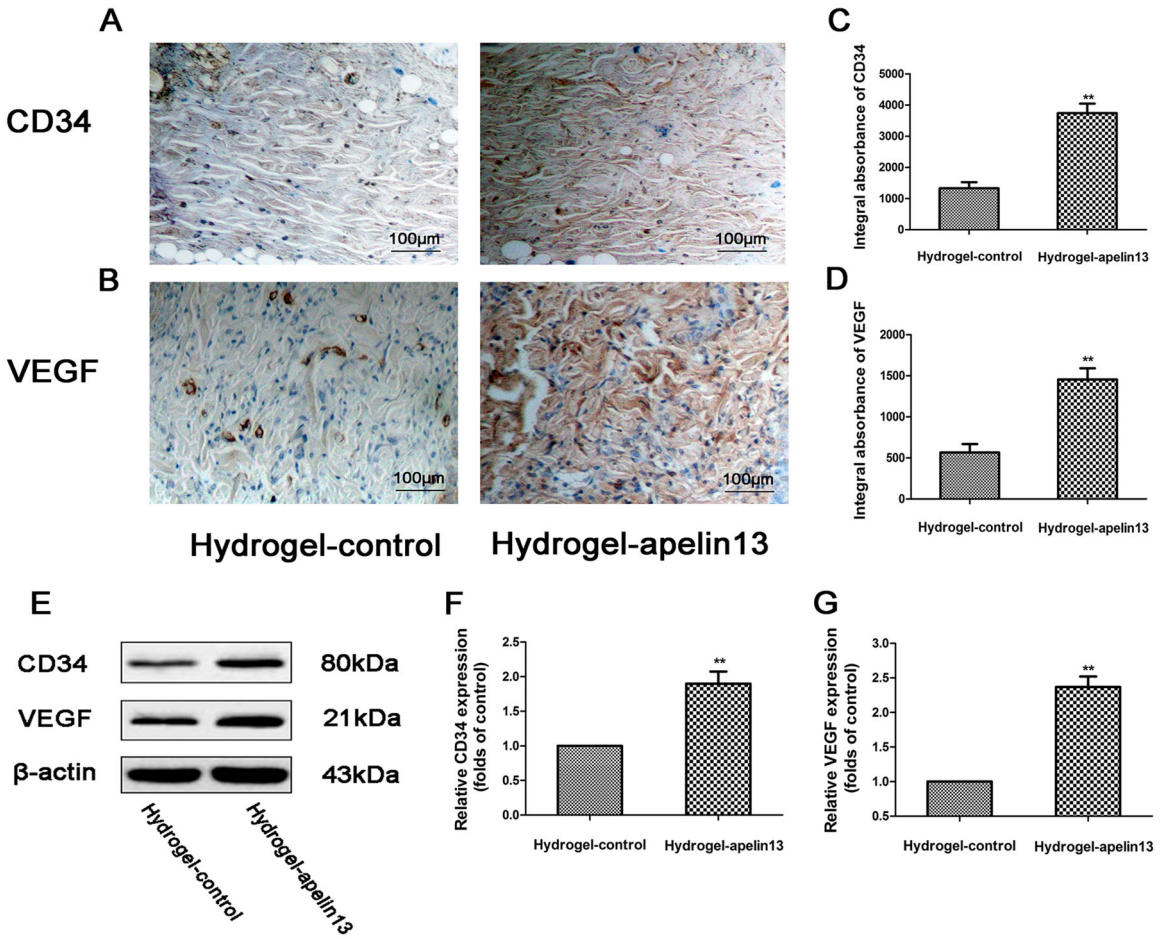

Fig. 6 Effect of CH/β-GP/apelin-13 hydrogel on CD34 and VEGF expression. **a**, **b** CD34 and VEGF expression in the control hydrogel group and apelin-13 hydrogel group was detected through immunohistochemistry staining. **c**, **d** The integral absorbance value of CD34 and VEGF in the two groups. **e**, **f** Western blot analysis was used to detect the protein expression of CD34 and VEGF in the two groups. $*p < 0.05$ and $**p < 0.01$ in comparison with the control group. Data represent mean values ± SD, $n = 6$ per group

significantly enhances the random skin flap survival. In addition, our studies revealed that its pharmacological mechanism of action involved dampening oxidative stress, promoting angiogenesis, and suppressing inflammation.

Recently, thermosensitive gel-forming systems have gained increasing attention as wound repair due to their advantages, such as easy preparation, low cost, low toxicity, eases of use and controlled release [14, 15]. In particular, the injectable and thermosensitive hydrogels is capable to fill up the skin defects and necrosis caused by random flap through a simple injection of the pre-gel solution. In the present study, an apelin-13-loaded CH/β-GP hydrogel was developed for promoting random skin flap survival. As shown in Fig. 2a, at 32 °C, the modulus of the CH/β-GP/apelin-13 solution changed dramatically, and was characterized by G′ (elastic modulus) outweighing G″ (viscous modulus). These results suggest that CH/β-GP/apelin-13 is a kind of thermo-sensitive hydrogel, and that the sol-gel transition could be triggered below or at body temperature. Furthermore, according to Fig. 2c, apelin-13 could be released from CH/β-GP/apelin-13 in a sustained manner, potentially due to the porous inner structure (Fig. 2b) and moist topical environment.

Improving angiogenesis and enhancing blood supply to ischemic areas was strongly considered to enhance the proportion of rats with random skin flap surviving, which was closely related to VEGF [30]. VEGF is a growth factor produced by platelets that modulates vascular endothelial cells, thereby accelerating regeneration and proliferation [31]. Several studies have revealed the function of VEGF in endothelial cells' activities such as proliferation. VEGF promotes revascularization and blood supply to the ischemic flaps, thus increasing flap survival [32, 33]. In this study, the VEGF expression level was markedly higher in apelin-13 hydrogel group than those in the control hydrogel group. Our findings agree with previous studies that reported that apelin-13 notably elevated the protein quantity of VEGF in stroke mice [11]. Furthermore, the MVD, a marker of angiogenesis, was much larger in apelin-13 hydrogel group than control group. Moreover, the results of

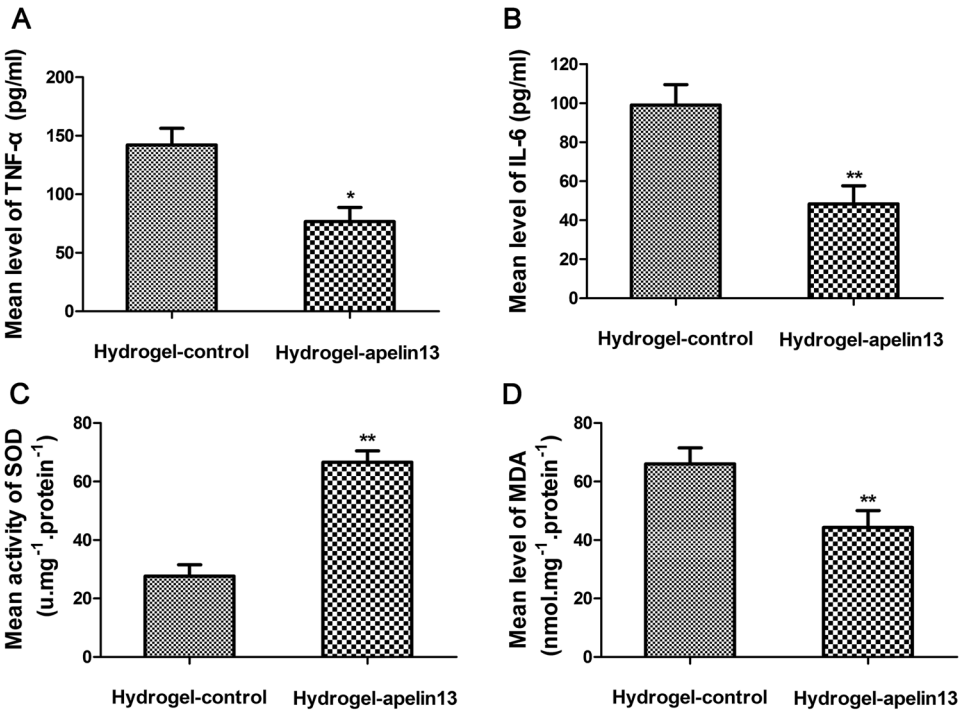

Fig. 7 Effects of CH/β-GP/apelin-13 hydrogel on proinflammatory cytokines. **a**, **b** TNF-α and IL-6 expression in the control hydrogel group and apelin-13 hydrogel group was detected by ELISAs. **c** SOD activity in the two groups was measured by the oxidase enzymatic method. **d** MDA level in the two groups was gauged through an approach triggered by a reaction with thiobarbituric acid. $*p < 0.05$ and $**p < 0.01$ in comparison with the control group. Data represent mean values ± SD, $n = 6$ per group

doppler ultrasound showed that the apelin-13-treated flap exhibited visibly more blood flow than control group. However, flap water content was remarkably reduced in apelin-13-treated flap in comparison to the control group. All of the results indicate that apelin-13 may promote flap survival via VEGF-induced angiogenesis and facilitating detumescence.

Inflammatory response plays a fundamental role in the survival of random skin flaps [34]. Moderate coagulative necrosis with inflammatory cell infiltration is evident in the epidermis of random skin flaps. The greater the extent of necrosis, the more pronounced the inflammation, which compromises flap success [35]. Apelin-13 has been shown to possess anti-inflammatory activities in multifarious diseases such as myocardial infarction, spinal cord injury and ischemic stroke [36–38]. In the present study, TNF-α and IL-6 expressions were evidently decreased in the ischemic flap tissue after treatment with apelin-13. The results are consistent with Chen et al.'s results [11]. They found that apelin-13 treatment significantly suppressed the elevation of TNF-α and IL-6 after stroke in mice. Thus, we conclude that apelin-13 exerted potent anti-inflammatory effects in ischemic areas of random skin flaps.

It has been demonstrated that ischemia–reperfusion injury is characterized by endothelium/leukocyte interactions, oxygen free radicals, apoptosis, platelet aggregation, and is caused by acute disruption of blood-flow to the microvasculature [39]. MDA is produced following ischaemia-reperfusion injury. Its production can also aggravate cell membrane damage. Therefore, MDA content is a commonly used index in senescence physiology and resistance physiology research. MDA can be used to understand the extent of ischaemia-reperfusion injury, and indirectly measure the degree of membrane system damage and tissue stress resistance [35, 40]. SOD is a crucial antioxidant enzyme in organisms and the primary substance to scavenge free radicals in vivo. The level of SOD is a sensitive indicator of antioxidant status [41]. It was shown to inactivate O^{2-}, the precursor of H_2O_2 and OH^- and protect tissues against toxic oxygen-free radicals [42]. Therefore, the activity SOD and MDA content are crucial biomarkers of oxidative stress status. Here, MDA levels were lower and SOD activity was higher in apelin-13-treated flaps than controlled. The present results were partially in line with those reported by Boal et al. [43]. They reported that apelin-13 treatment significantly attenuated hypoxia-induced ROS overproduction, mitochondrial O^{2-} and H_2O_2 levels in cardiomyocytes isolated from high fat diet-fed mice. Collectively, these findings demonstrate that apelin-13 promoted flap survival may be through suppressing oxidative stress in random skin flaps.

Up to now, many pharmacological agents have been investigated for their effectiveness in preventing or reversing ischemia in skin flaps, such as vinpocetine [44], polydeoxyribonucleotide [45], naringin [46] and traditional Chinese medicine (Shuxuetong and Huangqi) [47, 48]. However, these agents need to injection or oral administration everyday because of their low plasma concentration and short half-life period. Also, the biosecurity of them is still unknown. On the contrary, our CH/β-GP/apelin-13

hydrogel only need to intradermal injection once in the areas of the flap after the surgical procedure. It could keep significantly higher plasma concentration in rat's body. Besides, CH/β-GP/apelin-13 hydrogel has better biosecurity as apelin-13 is an endogenous peptide. On the other hand, the good biocompatibility and biodegradability of CH/β-GP/apelin-13 hydrogel makes it more beneficial to clinical application.

However, the exact mechanism of apelin-13 on the improved flap survival in random skin flap was not settled. It was a shortcoming in this study. Further work is encouraged to explore the precise mechanism of the regulation of apelin-13 in the enhancement of flap survival in random skin flap.

5 Conclusion

In conclusion, in the present study, a new CH/β-GP/apelin-13 hydrogel is presented which has good applicability due to its biocompatibility and biodegradability in rat random pattern skin flap model. It was demonstrated to improve the random skin flap survival through increasing angiogenesis, suppressing inflammatory response and depressing oxidative stress. In summary, these results manifest that this CH/β-GP/apelin-13 hydrogel holds huge potential as an effective treatment choice for random pattern skin flap in the future.

Acknowledgements This study was supported by the Zhejiang Medical and Health Science and Technology Plan Project (No. 2017KY480) and National Natural Science Foundation of China (No. 81701928).

Compliance with ethical standards

Conflict of interest The authors declare that they have no conflict of interest.

References

1. Sen H, Oruc M, Isik VM, Sadic M, Sayar H, Citil R et al. The effect of omeprazole usage on the viability of random pattern skin flaps in rats. Ann Plast Surg. 2017;78:e5–e9.
2. Kailiang Z, Yihui Z, Dingsheng L, Xianyao T. Effects of muscone on random skin flap survival in rats. J Reconstr Microsurg. 2016;32:200–7.
3. Cao B, Wang L, Lin D, Cai L, Gao W. Effects of lidocaine on random skin flap survival in rats. Dermatol Surg. 2015;41:53–8.
4. Yang M, Sheng L, Li H, Weng R, Li QF. Improvement of the skin flap survival with the bone marrow-derived mononuclear cells transplantation in a rat model. Microsurgery. 2010;30:275–81.
5. Kim HJ, Xu L, Chang KC, Shin SC, Chung JI, Kang D et al. Anti-inflammatory effects of anthocyanins from black soybean seed coat on the keratinocytes and ischemia-reperfusion injury in rat skin flaps. Microsurgery. 2012;32:563–70.
6. Lima LP, de Oliveira Albuquerque A, de Lima Silva JJ, Medeiros F, de Vasconcelos PR, Guimaraes SB. Electroacupuncture attenuates oxidative stress in random skin flaps in rats. Aesthetic Plast Surg. 2012;36:1230–5.
7. Lee DK, Cheng R, Nguyen T, Fan T, Kariyawasam AP, Liu Y et al. Characterization of apelin, the ligand for the APJ receptor. J Neurochem. 2000;74:34–41.
8. Sandal S, Tekin S, Seker FB, Beytur A, Vardi N, Colak C et al. The effects of intracerebroventricular infusion of apelin-13 on reproductive function in male rats. Neurosci Lett. 2015;602:133–8.
9. Tatemoto K, Hosoya M, Habata Y, Fujii R, Kakegawa T, Zou MX et al. Isolation and characterization of a novel endogenous peptide ligand for the human APJ receptor. Biochem Biophys Res Commun. 1998;251:471–6.
10. Hosoya M, Kawamata Y, Fukusumi S, Fujii R, Habata Y, Hinuma S et al. Molecular and functional characteristics of APJ. Tissue distribution of mRNA and interaction with the endogenous ligand apelin. J Biol Chem. 2000;275:21061–7.
11. Chen D, Lee J, Gu X, Wei L, Yu SP. Intranasal delivery of Apelin-13 is neuroprotective and promotes angiogenesis after ischemic stroke in Mice. ASN Neuro. 2015;7:1759091415605114.
12. Yang Y, Zhang X, Cui H, Zhang C, Zhu C, Li L. Apelin-13 protects the brain against ischemia/reperfusion injury through activating PI3K/Akt and ERK1/2 signaling pathways. Neurosci Lett. 2014;568:44–9.
13. Yang S, Li H, Tang L, Ge G, Ma J, Qiao Z et al. Apelin-13 protects the heart against ischemia-reperfusion injury through the RISK-GSK-3beta-mPTP pathway. Arch Med Sci. 2015;11:1065–73.
14. Merino S, Martin C, Kostarelos K, Prato M, Vazquez E. Nanocomposite hydrogels: 3D Polymer-nanoparticle synergies for on-demand drug delivery. ACS Nano. 2015;9:4686–97.
15. Li Z, Guan J. Thermosensitive hydrogels for drug delivery. Expert Opin Drug Deliv. 2011;8:991–1007.
16. Li J, Shu Y, Hao T, Wang Y, Qian Y, Duan C et al. A chitosan-glutathione based injectable hydrogel for suppression of oxidative stress damage in cardiomyocytes. Biomaterials. 2013;34:9071–81.
17. Supper S, Anton N, Seidel N, Riemenschnitter M, Curdy C, Vandamme T. Thermosensitive chitosan/glycerophosphate-based hydrogel and its derivatives in pharmaceutical and biomedical applications. Expert Opin Drug Deliv. 2014;11:249–67.
18. Qu Y, Tang J, Liu L, Song L, Chen S, Gao Y. Alpha-tocopherol liposome loaded chitosan hydrogel to suppress oxidative stress injury in cardiomyocytes. Int J Biol Macromol. 2019;125:1192–202.
19. Kim S, Nishimoto SK, Bumgardner JD, Haggard WO, Gaber MW, Yang Y. A chitosan/beta-glycerophosphate thermo-sensitive gel for the delivery of ellagic acid for the treatment of brain cancer. Biomaterials. 2010;31:4157–66.
20. Zhao Y, Liu JG, Chen WM, Yu AX. Efficacy of thermosensitive chitosan/beta-glycerophosphate hydrogel loaded with beta-cyclodextrin-curcumin for the treatment of cutaneous wound infection in rats. Exp Ther Med. 2018;15:1304–13.
21. Peng H, Huang Q, Yue H, Li Y, Wu M, Liu W et al. The anti-tumor effect of cisplatin-loaded thermosensitive chitosan hydrogel combined with radiotherapy on nasopharyngeal carcinoma. Int J Pharm. 2019;556:97–105.
22. Chenite A, Chaput C, Wang D, Combes C, Buschmann MD, Hoemann CD et al. Novel injectable neutral solutions of chitosan form biodegradable gels in situ. Biomaterials. 2000;21:2155–61.
23. McFarlane RM, Deyoung G, Henry RA. The design of a pedicle flap in the rat to study necrosis and its prevention. Plast Reconstr Surg. 1965;35:177–82.

24. Tao XY, Wang L, Gao WY, Ding J, Feng XL, Zhou ZW et al. The effect of inducible nitric oxide synthase on multiterritory perforator flap survival in rats. J Reconstr Microsurg. 2016;32:643–9.
25. Shi ZR, Itzkowitz SH, Kim YS. A comparison of three immunoperoxidase techniques for antigen detection in colorectal carcinoma tissues. J Histochem Cytochem. 1988;36:317–22.
26. Ozkan F, Senayli Y, Ozyurt H, Erkorkmaz U, Bostan B. Antioxidant effects of propofol on tourniquet-induced ischemia-reperfusion injury: an experimental study. J Surg Res. 2012;176:601–7.
27. Lin Y, Lin B, Lin D, Huang G, Cao B. Effect of thymosin beta4 on the survival of random skin flaps in rats. J Reconstr Microsurg. 2015;31:464–70.
28. Reichenberger MA, Heimer S, Schaefer A, Lass U, Gebhard MM, Germann G et al. Extracorporeal shock wave treatment protects skin flaps against ischemia-reperfusion injury. Injury. 2012;43:374–80.
29. Beeres SL, Bengel FM, Bartunek J, Atsma DE, Hill JM, Vanderheyden M et al. Role of imaging in cardiac stem cell therapy. J Am Coll Cardiol. 2007;49:1137–48.
30. Basu G, Downey H, Guo S, Israel A, Asmar A, Hargrave B et al. Prevention of distal flap necrosis in a rat random skin flap model by gene electro transfer delivering VEGF(165) plasmid. J Gene Med. 2014;16:55–65.
31. Kalka C, Tehrani H, Laudenberg B, Vale PR, Isner JM, Asahara T et al. VEGF gene transfer mobilizes endothelial progenitor cells in patients with inoperable coronary disease. Ann Thorac Surg. 2000;70:829–34.
32. Zhang F, Fischer K, Komorowska-Timek E, Guo M, Cui D, Dorsett-Martin W. et al. Improvement of skin paddle survival by application of vascular endothelial growth factor in a rat TRAM flap model. Ann Plast Surg. 2001;46:314–9.
33. Zhang F, Lineaweaver W. Acute and sustained effects of vascular endothelial growth factor on survival of flaps and skin grafts. Ann Plast Surg. 2011;66:581–2.
34. Kuo YR, Wu WS, Hsieh YL, Wang FS, Wang CT, Chiang YC et al. Extracorporeal shock wave enhanced extended skin flap tissue survival via increase of topical blood perfusion and associated with suppression of tissue pro-inflammation. J Surg Res. 2007;143:385–92.
35. Zhou KL, Zhang YH, Lin DS, Tao XY, Xu HZ. Effects of calcitriol on random skin flap survival in rats. Sci Rep. 2016;6:18945.
36. Chung WJ, Cho A, Byun K, Moon J, Ge X, Seo HS et al. Apelin-13 infusion salvages the peri-infarct region to preserve cardiac function after severe myocardial injury. Int J Cardiol. 2016;222:361–7.
37. Wang K, Ju Z, Yong Y, Chen T, Song J, Zhou J. The effects of electroacupuncture on the Apelin/APJ System in the spinal cord of rats with inflammatory pain. Anesth Analg. 2016;123:1603–10.
38. Xin Q, Cheng B, Pan Y, Liu H, Yang C, Chen J et al. Neuroprotective effects of apelin-13 on experimental ischemic stroke through suppression of inflammation. Peptides. 2015;63:55–62.
39. Kim EK, Hong JP. The effect of recombinant human erythropoietin on ischemia-reperfusion injury: an experimental study in a rat TRAM flap model. Plast Reconstr Surg. 2007;120:1774–81.
40. Taleb S, Moghaddas P, Rahimi Balaei M, Taleb S, Rahimpour S, Abbasi A et al. Metformin improves skin flap survival through nitric oxide system. J Surg Res. 2014;192:686–91.
41. He F, Li J, Liu Z, Chuang CC, Yang W, Zuo L. Redox mechanism of reactive oxygen species in exercise. Front Physiol. 2016;7:486.
42. Sirota TV, Zakharchenko MV, Kondrashova MN. Cytoplasmic superoxide dismutase activity is a sensitive indicator of the antioxidant status of the rat liver and brain. Biomed Khim. 2014;60:63–71.
43. Boal F, Timotin A, Roumegoux J, Alfarano C, Calise D, Anesia R et al. Apelin-13 administration protects against ischaemia/reperfusion-mediated apoptosis through the FoxO1 pathway in high-fat diet-induced obesity. Br J Pharm. 2016;173:1850–63.
44. Xiao-Xiao T, Sen-Min W, Ding-Sheng L. Effects of vinpocetine on random skin flap survival in rats. J Reconstr Microsurg. 2013;29:393–8.
45. Chung KI, Kim HK, Kim WS, Bae TH. The effects of polydeoxyribonucleotide on the survival of random pattern skin flaps in rats. Arch Plast Surg. 2013;40:181–6.
46. Cheng L, Chen T, Tu Q, Li H, Feng Z, Li Z et al. Naringin improves random skin flap survival in rats. Oncotarget. 2017;8:94142–50.
47. Cai L, Huang W, Lin D. Effects of traditional Chinese medicine Shuxuetong injection on random skin flap survival in rats. ScientificWorldJournal. 2014;2014:816545.
48. Cai L, Cao B, Lin D. Effects of traditional chinese medicine huangqi injection (Radix astragali) on random skin flap survival in rats. J Reconstr Microsurg. 2015;31:565–70.